An Approach to Increase the Battery Time of a Mobile Phone Using Free Energy Harvesting

Kirkegaard Jensen, Jesper; Jessen, Kasper; Laugesen, Kasper; Mortensen, Signe Møller; Bech Sørensen, Juliane; Forouzbaksh, Farshid

Published in:
Proceedings of the 2015 IEEE International Telecommunications Energy Conference (INTELEC)

DOI (link to publication from Publisher):
10.1109/INTLEC.2015.7572478

Publication date:
2015

Document Version
Early version, also known as pre-print

An Approach to Increase the Battery Time of a Mobile Phone Using Free Energy Harvesting

Jesper Kirkegaard Jensen, Kasper Jessen, Kasper Laugesen, Signe Møller Mortensen, Juliane Bech Sørensen
Farshid Forouzbakhsh
Department of Energy Technology, Aalborg University, Denmark

***Abstract*—The increasing market of mobile phones, has increased the need for electricity to power mobile phones, as well. This paper investigates the possibilities to charge a mobile phone by harvesting energy from the surroundings. Some technologies are better suited for this purpose than others. Through previous analyses solar cells and electromagnetic generator were found to be the most suitable solution. This paper will give a basic description of the operating conditions of solar cells and an electromagnetic generator. There will also be a short view on the electrical circuit needed for implementing the harvested energy. Calculations regarding the power produced by amorphous silicon solar cells in both sun light and light from different light emitting sources will be examined. Furthermore calculations of the spring for the electromagnetic generator and the power produced by this device will be examined.**
Through experiments and data processing the energy delivered by the solar cells and the electromagnetic generator is investigated, furthermore an experiment regarding the movement of the phone will be executed.

I. Introduction

Most new smart phones today do not have a long battery life, before they need to recharge, this might be a problem to users not able to charge their mobile phone using regular chargers for a longer period of time. Therefore a lot of research has been done to increase the battery capacity.
This paper wants to look at this problem in a different way. Instead of increasing the battery capacity, the battery life of a mobile phone can be extended using a portable energy harvesting device, which makes use of the natural resources available from the surroundings.

Different technologies were analysed in order to obtain the most suitable solution. The technologies analysed include: wind turbines, which make use of the energy from the wind; solar cells which make use of the energy in light; the electrowetting property a material can posses and thereby transform energy from applied force to electrical energy; the piezoelectric effect occurring in some forms of materials creating dipole moments; a thermoelectric generator (TEG) creating current using temperature difference; static electricity which make use of the charge created by rubbing two different materials against each other and an electromagnetic generator (EMG) which make use of movements.

The following design requirements were set up in order to choose the most suitable technology:

- The size of the product should be able to fit in a pocket
- The product should be affordable
- The product may either be a part of a newly fabricated phone, or as an external cover for existing phones
- The product should be able to charge the mobile phone regardless of the type of surroundings
- The product should be able to charge the mobile phone when the user is stationary or when the user moves

Through analyses and comparisons of the different technologies a combined solution with solar cells and EMG seemed as a suitable combination fitting the requirements.
One possible design is to extend the phone internally to make room for the EMG. Another possibility is a cover with the EMG incorporated with a plug-in, while the solar cells would be placed as a sleeve around the phone.

II. Characteristics of Power Harvesting Applications

A. Basics of Solar Cells

There are two common types of solar cells; crystalline and thin film. The crystalline solar cells are the mature technology while the thin film solar cells have been developed during recent years. The main difference between these two is the semiconducting material. The crystalline solar cells are typically built of silicon wafers containing a single or more crystals, while the thin film solar cells are made by applying layers of the semiconducting material onto a plate of e.g. glass. [1]

Thin film amorphous silicon solar cells are used in this paper. The advantages of thin film solar cell include light weight, flexibility, integrity and they are cheap compared to the crystalline solar cells. The disadvantages include low efficiency and that their performance is dependent on the surrounding environment. [1]

Solar cells convert the energy from light into electrical energy. The energy from light is absorbed by electrons, thereby the electrons achieve a higher energy level. To make the electron able to move to an external circuit, it has to overcome a certain amount of energy, called the band gap, before being able to reach the conduction band. In the case of amorphous silicon the band gap is 1.7-1.8 eV. [2]

B. Basics of the Electromagnetic Vibration Harvester

An EMG to harvest vibrational energy is based on the electromagnetic induction principle described by Faraday's law, stating that an electrical current is induced in all closed

978-1-4799-6582-3/15/$31.00 ©2015 IEEE

circuits, when the magnetic flux through a surface bounded by the conductor changes.

The main advantages of EMGs are: low cost of production and high power density. The disadvantages are: their scaling power factor meaning that the output of the electromagnetic energy harvesters depends largely on their size, and that motion is needed to create the vibration. [3]

For creating the magnetic field, permanent magnets are used, and the conductor is often formed as a coil, while the varying magnetic field is created by vibration or motion. The most practical construction of the EMG is having the coil fixed to the frame, as the terminals are fixed and the magnet is less fragile compared to the coil. This results in the moving magnet principle. The relative movement is generally divided into two different types; the lateral movement between the magnet and coil, and the movement of the magnet in and out of the coil.

C. Electrical Circuit

In order to create a circuit able to handle the produced power between the energy harvester and the battery, different controlling and converting devices are needed. The devices of the circuit are:

- **Rectifier** The AC voltage produced by the EMG has to be rectified by a full wave rectifier in order to be able to charge the battery
- **Diode** To prevent that the power leaking from the battery to the solar cell a single diode is inserted
- **Buck/boost converter** The voltages produced by both the EMG module and the solar cells most often differ from the required charging voltage of the battery. Therefore the voltage has to be regulated in order to be able to charge the battery. This is done by a buck/boost converter, stepping the voltage down/up
- **Charging circuit** The system needs a charging circuit able to control the charging to avoid damaging the battery. This is most often integrated in the phone

These devices are connected, as seen in the block diagram in Fig. 1.

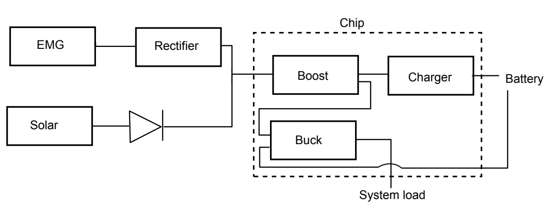

Figure 1: Block diagram of the different elements connected together

III. Modelling

A. Solar Cells

Not all wavelengths contain the amount of energy needed in order to overcome the band gap, while other wavelengths has to much energy, resulting in thermal waste. The band gap and wavelength are related by (1).

$$\lambda = \frac{hc}{E_g} \tag{1}$$

Where h is Planck's constant, c is the speed of light, while E_g is the band gap of the given material. For the case of amorphous silicon only wavelengths shorter than 729 nm will be able to move an electron to the conduction band. Thereby the performance of the solar cell is strongly dependent on the incident light. As the light, the solar cells are exposed to, will vary, the spectral intensity of different light emitting sources is investigated. The spectral intensity of the sun, an fluorescent light bulb, an incandescent light bulb and a halogen light bulb is seen in Fig. 2 by using the equation of a black body radiation (2)

$$F(\lambda) = \frac{2\pi hc^2}{\lambda^5 \left(\exp\left(\frac{hc}{\sigma\lambda T} - 1\right)\right)} \tag{2}$$

Where $F(\lambda)$ is the spectral intensity, λ is the wavelength and T is the colour temperature of the light emitting source.

The spectral intensity is highest for the sun and lowest for the incandescent light bulb. The black dotted line indicates the band gap of amorphous silicon. As the solar cells are placed some distance away from the light emitting source, this has to be considered, as well. The spectral intensity decays by the square of the distance, as seen in (3).

$$F_{scl} = \frac{r_s^2}{d^2} F_s \tag{3}$$

Where F_{scl} is the spectral irradiation the solar cell receives, r_s is the radius of the given light emitting source, which is the radius of the sun or an assumed radius of 2 mm in the case of the lamps. d is the mean distance between the sun and the solar cells or an assumed mean distance of 2 m between the light emitted from lamps and the solar cell. While F_s is the spectral irradiation emitted from the source. The different power densities for the light emitting sources were calculated and found in Table I.

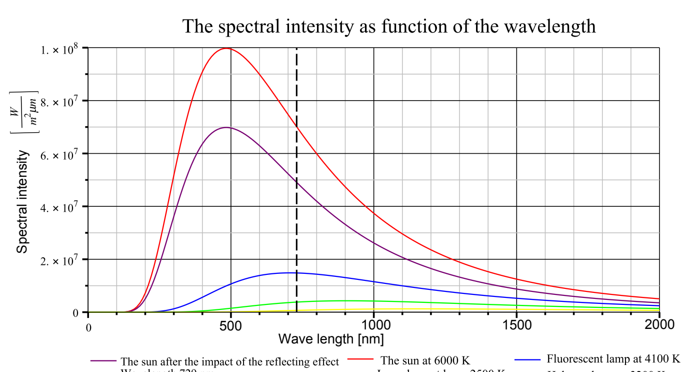

Figure 2: The spectral intensities of different light emitting sources

Table I: Power Densities of Light Emitting Sources

	Sun	Fluorescent	Halogen	Incandescent
P [W/m^2]	1.11k	16.0	5.95	2.21

By using the spectral intensity the short circuit current is found using (4) from [2].

$$I_{sc} = q\int_0^{\lambda_{max}} \frac{F(\lambda)\lambda}{hc} d\lambda \tag{4}$$

Where q is the elementary charge and λ_{max} is the maximum usable wavelength, which is given in (1). The current of a solar cell can be determined using (5) from [2]. Where the first term is the short circuit current, and the second term is the diode equation of a non-ideal diode, as a solar cell is modelled as a non-ideal diode. The last term is the loss due to imperfections in the solar cell and is called the shunt current.

$$I = I_{sc} - I_s\left(\exp\left(\frac{qV}{n\sigma T_s}\right)\right) - \frac{V}{R_{sh}} \tag{5}$$

Here I_s is the reverse saturation current, which is a material constant defining the amount of current flowing the reverse way through the solar cell. V is the voltage across the solar cell, n is the ideality factor, defining how close the solar cell is to an ideal diode. σ is Boltzmann's constant, T_s is the surface temperature of the solar cell, while R_{sh} is the shunt resistance. The IV-characteristic of the solar cell is seen in Fig. 3.

From these characteristics, parameters regarding the solar cell can be found. The open circuit voltage is found by (6) from [4].

$$V_{oc} = \frac{\sigma T_s}{q}\ln\left(\frac{I_{sc}}{I_s} + 1\right) \tag{6}$$

The maximum power current and voltage are reached when the power reaches maximum. At this point the load connected to the solar cell will equal the characteristic resistance of the solar cell. The efficiency of the solar cell is found by using (7).

$$\eta = \frac{V_{mp}I_{mp}}{P_{light}} \tag{7}$$

Where V_{mp} is the maximum power voltage, I_{mp} is the maximum power current, while P_{light} is the irradiation of the light emitting source. All these parameters are found in Table II.

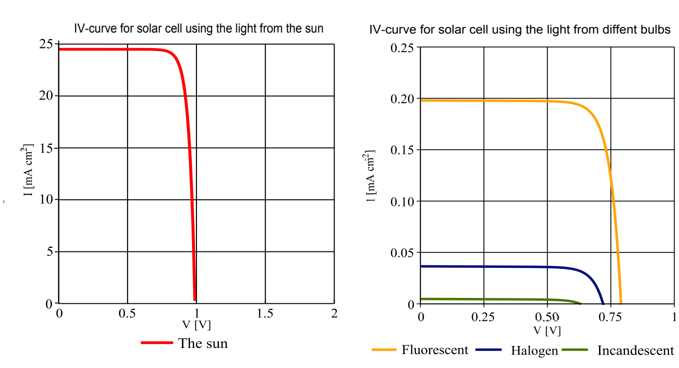

Figure 3: Theoretical IV-characteristics

Table II: Different Parameters Regarding Solar Cells

	Sun	Fluorescent	Halogen	Incandescent
I_{sc} [mA/cm^2]	24	0.20	0.036	0.0047
$V_{oc}[V]$	0.99	0.79	0.72	0.64
I_{mp} [mA/cm^2]	23	0.19	0.034	0.0039
V_{mp} [V]	0.86	0.67	0.61	0.52
P_{max} [mW/cm^2]	20	0.12	0.020	0.0020
R_{ch} [Ω]	37	3.6k	18k	0.13M
η [%]	18	7.8	3.4	0.92

Another parameter regarding solar cells is the absorption coefficient, which defines how far into a material a given wavelength can travel before being absorbed. This factor depends on the extinction coefficient, which indicates the amount of light a given material absorbs, and is given as the imaginary part of the refractive index. From this parameter the necessary thickness of the solar cell is determined, as the thickness is inverse proportional to the absorptions coefficient, which is given in (8) from [5].

$$\alpha = \frac{4\pi k}{\lambda} \tag{8}$$

Where k is the absorption coefficient. The absorption coefficient and the thickness of the solar cell are seen as the function of wavelength in Fig. 4. The black line at 729 nm indicates the band gap of amorphous silicon. The thickness can then be read as the point where the absorption depth crosses this line, and in this case it is 400 nm. This means the absorbing layer of the solar cell is able to absorb all the usable wavelengths to generate a current if it has a thickness of 400 nm.

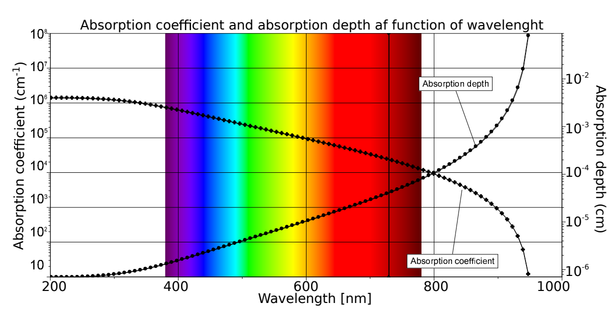

Figure 4: The absorption coefficient and depth varying with wavelength. Data from [5]

B. Electromagnetic Generator

The modelling of the system is illustrated in Fig. 5, where k is the spring constant, c is the damping coefficient of the damper and m is the mass of the oscillating magnet of 3.6 g.

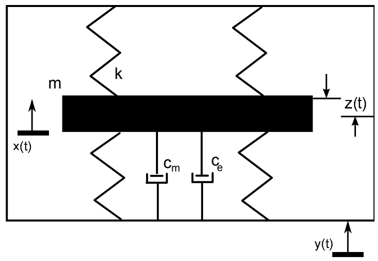

Figure 5: Model of a linear second order generator

$z(t)$ is the relative movement between base excitation movement, $y(t)$, and the movement of the oscillating magnet with respect to the frame, $x(t)$, as seen in (9).

$$z(t) = x(t) - y(t) \tag{9}$$

The dynamic model of the EMG is approximated as a linear second order mass-damper-spring system with a constant base excitation of a sinus signal: $y(t) = Y_i \sin(\omega t)$, as seen in (10).

$$0 = mx''(t) + cz'(t) + kz(t) \tag{10}$$

The damping of the mass spring system will be very small, and therefore an approximation, assuming the damping coefficient very small, c«1, is made. A calculation of the frequency is seen in (11).

$$\omega = \omega_n \sqrt{1 - \zeta^2} \tag{11}$$

Where ω_n is the natural frequency, and ζ is the damping ratio given by (12).

$$\zeta = \frac{c}{2\sqrt{mk}} \tag{12}$$

Thereby it can be approximated that $\omega \approx \omega_n$. The natural frequency is used to calculate the spring constant in (13).

$$k = \omega_n^2 m \tag{13}$$

The frequency is found by sampling data from the accelerometer inside a mobile phone while walking with the phone placed in the pocket. Only the vertical motion is taken into consideration, as it is assumed that most of the movement is in this direction. Therefore the EMG is designed for only making use of this movement. A series of test were made, and a graph of the most common acceleration is seen in Fig. 6.

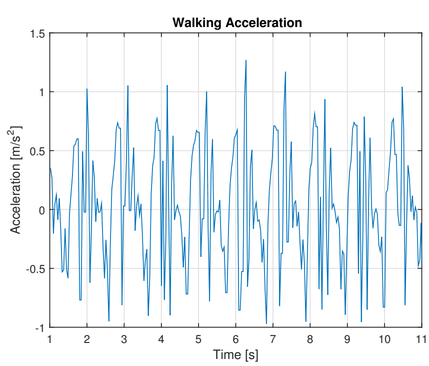

Figure 6: The acceleration of a mobile phone when walking

A repeating signal is observed in the figure. This signal can be found as a sum of sine functions, by analysing this signal using a Fast Fourier Transformation (FFT), the frequency spectrum shows that the highest amplitudes occur at 1.9 Hz in Fig. 7. An assumption of a sine wave with 1.9 Hz is used throughout the calculations for dimensioning the springs of the EMG. Now the spring constant can be calculated using (13) to be 3.6 $\cdot 10^{-3} \frac{N}{m}$ for each of the four springs.

Because of the gap between the magnet and the coil, a loss of magnetic field strength will occur. The magnetic field at the inside of the coil is calculated and assumed constant throughout the coil. The magnetic field strength from a rectangular magnet at a given distance, in this case 1 mm, is calculated by (14) from [6].

$$B_{cm} = \frac{b_r}{\pi}\left(sin^{-1}\left(\frac{l_m w_m}{4\sqrt{\left(\frac{w_m^2}{4}+z^2\right)\left(\frac{l_m^2}{4}+z^2\right)}}\right) - sin^{-1}\left(\frac{l_m w_m}{4\sqrt{\left(\frac{w_m^2}{4}+(z+h_m)^2\right)\left(\frac{l_m^2}{4}+(z+h_m)^2\right)}}\right)\right) \tag{14}$$

Where b_r is the residual magnetic field density of the magnet, l_m, h_m and w_m are the dimensions of the magnet which are 40 mm, 4 mm and 3 mm, respectively. l_{mc} is the gap between the magnet and the coil and B_{cm} is the magnetic field strength of the magnet at the coil, which is calculated to be 0.289 $\frac{N}{m \cdot A}$.

Damping of the system will consist of two parts; one from the mechanical part and one from the electrical part. The electrical damping is caused by the induction of the coil, and can be estimated by (15) from [7]:

$$c_e = \frac{(N\, B_{cm}\, h_c)^2}{R_{load} + R_{coil}} \tag{15}$$

R_{load} is the load connected to the EMG, which is equal to R_{coil} for maximum power. The electrical damping c_e is calculated to be 65.9 $\cdot$ 10^{-3} $\frac{N \cdot s}{m}$.

To find the mechanical damping, a limit is set up for the movement of the magnet. That is the displacement amplitude must not exceed $Z_{i,max}$ which is 8 mm.

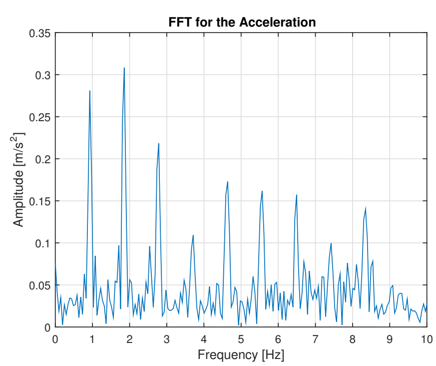

Figure 7: FFT of the acceleration of a mobile phone when walking

The amplitude is assumed to be from the bottom to the top of the coil, therefore a limit is needed otherwise the magnet would collide with the frame. This limit is used to calculate the mechanical damping coefficient able to withhold the limit of the amplitude in (16).

$$Z_{i,max} = \frac{mY_i\omega^2}{\sqrt{(k - m\omega^2)^2 + (c_e + c_m)^2\omega^2}} \tag{16}$$

Thereby the mechanical damping coefficient is calculated to be $6.1 \cdot 10^{-3}\ \frac{N \cdot s}{m}$.

The dynamic model in (10) with a base excitation as seen in Fig. 6, can now be simulated with respect to the movement of z. This is seen in Fig. 8.

As seen the damping in the system might be too high, as the movement will not reach the maximum amplitude of 8 mm. The open circuit generated voltage can be calculated by Faraday's law in (17).

$$e = -NBl\frac{dz}{dt} \tag{17}$$

Where e is the induced voltage, l is the length of one winding of the coil and $\frac{dz}{dt}$ is the velocity of the magnet.

The generated voltage was simulated and is shown in Fig. 9. With a load resistor with the same resistance as the coil of 414.1 Ω, the maximum power is found in Fig. 10.

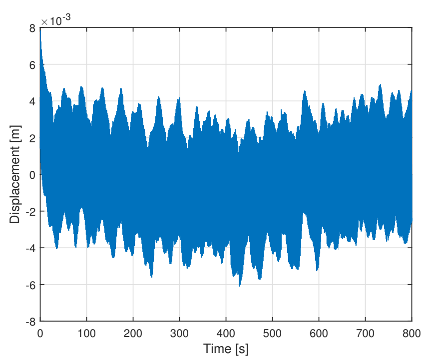

Figure 8: The movement of z as function of time

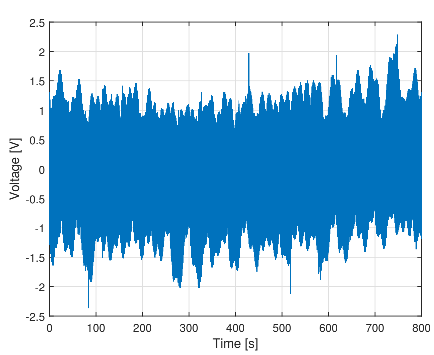

Figure 9: The voltage generated as function of time

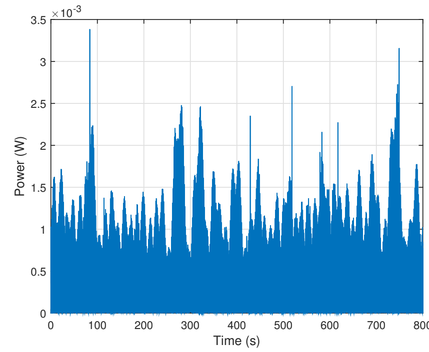

Figure 10: The power generated as function of time

IV. Experimental

A. Solar Cell

The solar cell tested were thin film amorphous silicon solar cells, and had a size of 11.4x15.0 cm and a thickness of 0.2 mm. The parameters regarding the solar cell, when exposed to the sun light, is found in Table III.

The solar cells were tested when exposed to light from a fluorescent lamp, with a measured power of 4.6 kW/m^2. The solar cell was placed 10 cm from the lamp and the open circuit voltage and short circuit current was measured. To get the IV-characteristic of the solar cell in Fig. 11, the load resistance was varied.

It is seen that the IV-characteristic is equivalent but not similar to Fig. 3, this is due to the shunt current, which has a bigger impact when the solar cells are used in light from lamps, causing the curve to flatten out.
Furthermore the power output vs. resistance was tested to find the characteristic resistance and maximum power of the solar cell at the given light. This is seen in Fig. 12.

Table III: Data from the Data Sheet of the Tested Solar Cells

I_{sc} [A]	V_{oc} [V]	I_{mp} [A]	V_{mp} [V]	P_{max} [W]	R_{ch}[Ω]	η[%]
0.12	8.0	0.10	6.0	0.6	60	3,5

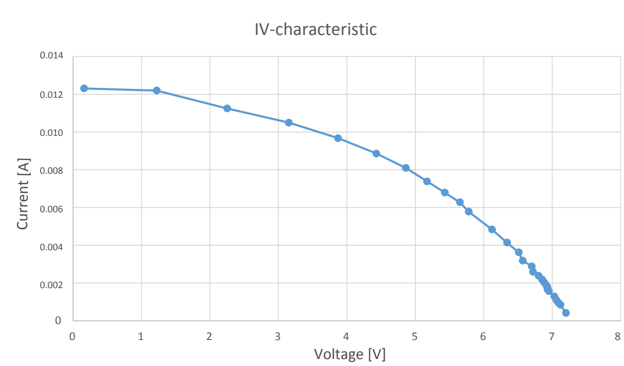

Figure 11: The IV-characteristic of the solar cell

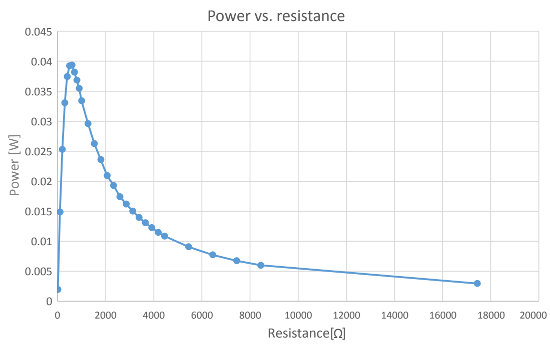

Figure 12: The power output and the load resistance

All the other parameters mentioned earlier can now be determined using these two graphs and are seen in Table IV.

If comparing this to the values of the data sheet seen in Table III, both the open circuit voltage and the maximum power voltage fit within an adequate margin, but the solar cells are tested in light from a fluorescent light bulb, while in the data sheet they are tested in light from the sun, making it difficult to compare the two outright. If comparing the currents, there is a big difference as the type of light emitting source is different. As seen in Fig. 2 the amount of usable wavelengths emitted from the fluorescent light bulb are small compared to the light emitted from the sun. The currents are approximately a factor of 10 to low compared to the data sheet, this means that the characteristic resistance has to be 10 times bigger if the power has to equal the data sheet. This is the case as the characteristic resistance in the data sheet is 60 Ω while the measured characteristic resistance is 600 Ω.

Table IV: Tested Solar Cells Using Florescent Light

I_{sc} [A]	V_{oc} [V]	I_{mp} [A]	V_{mp} [V]	P_{max} [W]	$R_{ch}[\Omega]$	$\eta[\%]$
0.012	7.3	8.1	0.005	0.039	600	0.057

B. Electromagnetic Generator

The EMG prototype consists of a rectangular coil with 1600 windings wound by a 100 μm copper wire and a neodymium magnet. The height of the coil is 16 mm, the inner length is 46 mm, the inner width is 6 mm, while the thickness of the coil is 2 mm. The measured resistance of the coil is 428 Ω, which is almost the same as the calculated of 414.1 Ω. The magnet consists of 2 rectangular bar neodymium magnets, each with a height of 4 mm, a length of 40 mm and a width of 3 mm. These two magnets were placed with identical poles attached to each other. The magnetic flux density was measured by a gauss-meter to be 0.3 $\frac{N}{m \cdot A}$ in a distance of 1 mm, which is approximately the same as the calculated magnetic flux density of 0.289 $\frac{N}{m \cdot A}$. The magnet was attached to the end of a rod, which was moved vertically in and out of the coil with a coupling of 1 mm. With a frequency of 2 Hz the voltage produced was measured by an oscilloscope in parallel with a 12 $k\Omega$ load resistor. From Fig. 13 it can be seen that the peak to peak voltage is 412 mV, while the calculated peak to peak voltage is approximately 3 V. This big difference in the peak to peak voltage is caused by the different resistor, as the resistor used in the calculations was a 414.1 Ω resistor. But as the voltage peaks were not measurable when using this resistance, a larger of 12 kΩ was inserted. Furthermore the experimental coil was being wound larger than calculated. The consequence of this is that the outer windings of the coil only contribute to a higher resistance, and not to induce a voltage, assuming the magnetic field does not reach these windings.

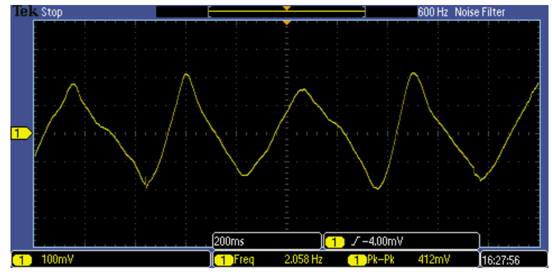

Figure 13: The voltage generated by the coil at a frequency of 2 Hz

V. Conclusion

To increase the battery life of a mobile phone using free energy harvesting the paper has presented a possible solution by usage of solar cells and EMG. The results showed that both solar cells and EMG were able to increase the battery life of a mobile phone. Solar cells used in sun light showed a power output significantly higher than the solar cells exposed to other light emitting sources. The results showed that a mobile phone would be charged fully if exposed to sun light all the time, but only extend the battery life by a couple of hours when used in florescent light and only a few minutes when used in light from an incandescent light bulb depending on the phone and usage of it.

Furthermore the results showed that the battery life could be extended for a short amount of time when using the EMG, based on the results from the walking of the user, and the assumption of the mobile phone being moved during the whole battery life. If this technology is to be used, the technology has to be researched and developed further, if a higher power output is desired.

References

[1] M. Pagliaro, R. Ciriminna, and G. Palmisano, *Flexible solar cells*. WILEY, Weinheim, 2008.

[2] J. Nelson, *The Physics of Solar Cells*, ser. Series on Properties of Semiconductor Materials.

[3] L. Kong, T. Li, H. Hng, F. Boey, T. Zhang, and S. Li, *Waste Mechanical Energy Harvesting*, ser. Lecture Notes in Energy. Springer Berlin Heidelberg, 2014.

[4] A. Shah, *Thin-Film Silicon Solar Cells*, ser. Engineering Sciences. EFPL Press, USA, 2010.

[5] P. E. F. Schubert, "Materials - refractive index and extinction coefficient," Cited 13-07-2015. [Online]. Available: http://homepages.rpi.edu/ schubert/

[6] J. Svoboda, *Magnetic Techniques for the Treatment of Materials*. Springer, 2004.

[7] M. El-hami, N. M. Glynne-Jones, M. White, S. Hill, E. Beeby, A. D. James, J. N. Brown, and Ross, "Design and fabrication of a new vibration-based electromechanical power generator," vol. 92, pp. 335–342, 2001.